

Guiding mode in elliptical core microstructured polymer optical fiber

Yani Zhang (张亚妮)^{1,2,3}, Liyong Ren (任立勇)², Kang Li (李康)², Hanyi Wang (王韩毅)², Wei Zhao (赵卫)², Lili Wang (王丽莉)², Runcai Miao (苗润才)³, Maryanne C. J. Large⁴, and Martijn A. van Eijkelenborg⁴

¹Department of Physics, Baoji College of Arts & Science, Baoji 721007

²State Key Laboratory of Transient Optics and Photonics, Xi'an Institute of Optics and Precision Mechanics, Chinese Academy of Sciences, Xi'an 710068

³Institute of Physics and Information Technology, Shaanxi Normal University, Xi'an 710062

⁴Optical Fibre Technology Centre, University of Sydney, 206 National Innovation Centre, NSW 1430, Australia

Received September 26, 2006

A kind of microstructured polymer optical fiber with elliptical core has been fabricated by adopting *in-situ* chemical polymerization technology and the secondary sleeving draw-stretching technique. Microscope photography demonstrates the clear hole-structure retained in the fiber. Though the holes distortion is visible, initial laser experiment indicates that light can be strongly confined in the elliptical core region, and the mode field is split obviously and presents the multi-mode characteristic. Numerical modeling is carried out for the real fiber with the measured parameters, including the external diameter of 150 μm , the average holes diameter of 3.3 μm , and the average hole spacing of 6.3 μm by using full-vector plane wave method. The guided mode fields of the numerical simulation are consistent with the experiment result. This fiber shows the strong multi-mode and weak birefringence in the visible and near-infrared band, and has possibility for achieving the fiber mode convertors, mode selective couplers and so on.

OCIS codes: 060.2310, 060.2280, 060.2290, 060.2270.

Microstructured optical fibers (MOFs), also known as "photonic crystal" or "holey" fibers, produce their light guidance effects through a pattern of tiny holes which run along the entire length of the fibers^[1]. Depending on the holes pattern, the photonic crystal fibers (PCFs) can be designed to display a diverse range of behaviors compared with conventional fibers, offering strong potential for a wide variety of photonic devices. For example, they can be made endlessly single-mode^[2], have either very large or small nonlinearity^[3], and have unusual dispersion characteristics such as ultra-flat dispersion^[4]. By defecting one or more air holes in the core regions of the fibers, it is also possible to make them have highly birefringent effect or multi-core bend sensing and twin-core strain sensing effect^[5–8].

However, most works have been concentrated on silica fibers, where the preform is produced by capillary stacking^[1,2] or casting using sol-gel techniques. More recently MOFs have been made in polymer^[9] because microstructured polymer optical fibers (mPOFs) offer the potential to fabricate fiber with an almost limitless range of internal holes structures^[10]. The degree of structural freedom is the result of the availability of a range of preform fabrication methods and the diversity of suitable polymeric materials (many of which can be readily doped and chemically modified). These advantages together with the relatively low draw temperatures associated with polymers result in mPOFs actively investigated as an alternative to microstructured glass optical fibers for specific application.

Unlike silica PCFs generally fabricated by stacking an array of silica capillaries and rods, mPOF preform can be

made by a variety of techniques, for example by drilling the desired pattern of holes in commercial poly-methyl methacrylate (PMMA) preform, or by casting mould of preform, by extruding PMMA preform rods and then drawing the preform into fibers^[11]. These methods allow for more complex designs potentially. In this paper, by *in-situ* chemical polymerization of preform^[12] and the secondary sleeving draw-stretching technique, an elliptical core mPOF was fabricated by removing triple adjacent air holes in core regions from a periodic triangular lattice hexangular structure fiber. The initial laser experiment indicates an interesting phenomenon of guiding mode in this fiber, which is according with the results of the numerical simulation for the real fiber by using full-vector plane wave method (FV-PWM).

Our fabrication procedure can be described as follows^[13]. Firstly, a mixed solution of methyl methacrylate (MMA) containing a specific amount of *t*-butyl peroxy isopropylcarbonate as the polymerization initiator, *n*-butyl mercaptan as a chain transfer reagent was prepared. Secondly, the mixed solution was pre-polymerization at 80 °C for about 3 hours and poured into a mould that mirrors the required preform holes structure. Thirdly, the polymerization was implemented at oven for about 72 hours from polymerization starting at 60 °C to the end at 185 °C to form the preform, with the length of 35 cm and the diameter of 7 cm. And then is the preform obtained was heat-drawn directly to shape the secondary preform with 15-mm diameter at 190 °C. Lastly, the secondary preform was sleeved with internal diameter of 15 mm and stretched into the fiber of 150 μm at the temperature of 225–228 °C and the steady

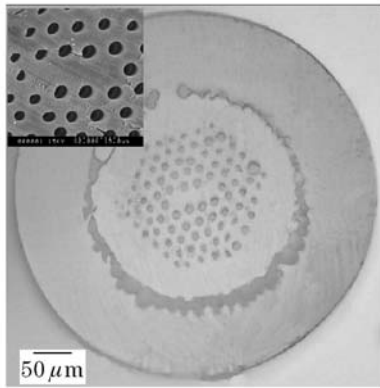


Fig. 1. SEM images of the elliptical mPOF cross-section and close-up of the core region (inset).

drawing tension of 100 g. The scanning electron microscope (SEM) image of the fibers obtained is shown in Fig. 1. The dark circle ring is an interface between the fiber cladding and the sleeve, which is used to protect outside hole-microstructure^[14]. The closed-up of the fiber core region (inset) indicates that the fiber has an average hole-diameter $d = 3.3 \mu\text{m}$ and hole-spacing $\Lambda = 6.3 \mu\text{m}$. Because of collapse of the holes during fiber drawing, the fiber structure is not uniform, and some deformations are visible, such as the holes diameter and the holes shape, and some of them even have elliptical shapes. Compared with the preform rods that the fiber was drawn from, the hole structure in the fiber has slightly increased in the ratio of hole-diameter and hole-spacing, $d/\Lambda = 0.52$, whereas in the preform rods $d/\Lambda = 0.4$. It can be observed from the SEM image that the designed holes structure is fully remained in the fiber sample, we determined the holes-spacing Λ and holes-diameter d by the average values from the first to the third rings of holes, and the error is about $\pm 5\%$.

It is well known that V-parameter determines the number of guiding mode. For photonic crystal fiber, the V-parameter is defined as^[15]

$$V_{\text{PCF}}(\lambda) = \frac{2\pi\Lambda}{\lambda} [n_c(\lambda)^2 - n_{\text{cl}}(\lambda)^2]^{1/2}, \quad (1)$$

where $n_c(\lambda)$ is the effective index of the fundamental mode associated with the index of the core, and similarly, $n_{\text{cl}}(\lambda)$ is the effective index of the fundamental space-filling mode in the triangular lattice cladding. With the measured parameters of the sample fiber, numerical simulations are presented by using FV-PWM^[16]. Figure 2 shows the dependence of V-parameter on normalized frequency (left axis), it can be seen that the cut-off wavelength of the fundamental mode is about $\lambda^* = 1310 \text{ nm}$ according to the condition of $V_{\text{PCF}} = \pi$. Because of the relative hole diameter of the sample fiber $d/\Lambda = 0.52$, the mPOF with elliptical core should support higher-order mode at wavelength $\lambda < \lambda^*$ ^[15]. Figure 2 shows the dependence of fundamental mode birefringence on normalized frequency (right axis). It can be seen the birefringence is strong at $\lambda > \lambda^*$ (region of the single-mode). Contrarily, the birefringence is weak at $\lambda < \lambda^*$ (region of the multi-mode).

To clarify the nature of the multimode, we investigated the spatial structure of the modes propagating in 1.2-m

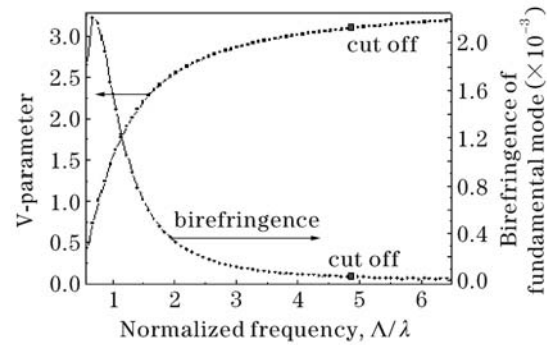


Fig. 2. Dependences of V-parameter on normalized frequency and fundamental mode birefringence on normalized frequency. Square shows cutoff wavelength.

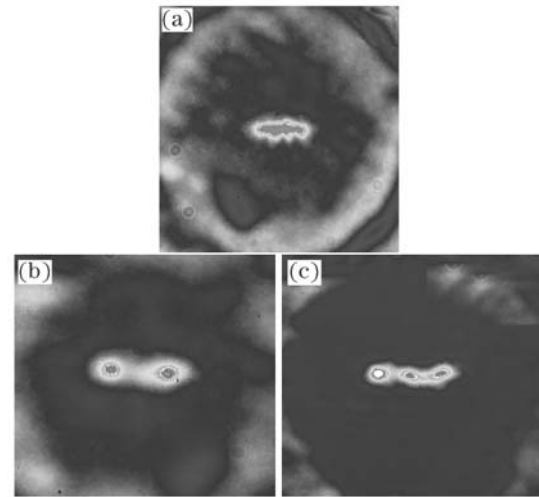


Fig. 3. Near-field images recorded at the output of 1.2-m fiber. (a) Fundamental mode at 980 nm, (b) and (c) higher-order modes at 980 nm.

fiber at 980 nm. In the experimental setup, the laser light with wavelength of 980 nm generated by semiconductor laser was launched into the fiber sample through collimating and focusing by a pair of $\times 10$ object lens. The output beam was detected with a charge coupled device (CCD) camera connected to optical spectral analyzer (OSA). The patterns observed were summarized in Fig. 3. It is clear that the guided mode is very well confined to the core region and presents an obvious ellipse. Figure 3(a) shows that it is possible to excite a fundamental mode with a maximum in the middle of the core. Two higher-order modes including the second-order mode and third-order mode with a minimum in the middle of the core are plotted in Figs. 3(b) and (c), respectively.

The calculated spatial guiding mode fields at the same wavelength are also shown in Fig. 4. The results of simulations show the mode indices of the six lower-ordered modes group two by two. The mode distribution of the first group is plotted in Fig. 4(a) which shows the similar spatial intensity structure of Fig. 3(a), we can consider that this mode field distribution corresponds to fundamental mode. Because of the mPOF with elliptical core is twofold symmetrical, the presence of a form asymmetry in fiber is supported by the birefringence caused by the refractive index difference of the fundamental modes,

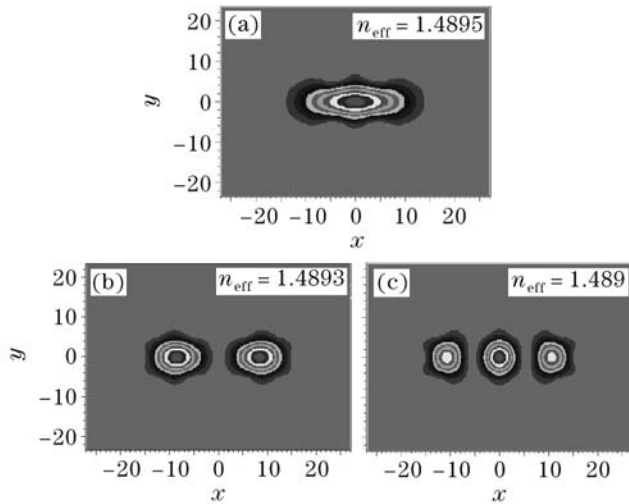


Fig. 4. Calculated mode profiles and effective indices of the mPOF for (a) the fundamental mode, (b) and (c) higher-order modes.

theoretical simulation indicates that the corresponding refractive index difference is $\Delta n = 2.9 \times 10^{-5}$ at cut-off wavelength of 1310 nm. It can be found from Fig. 2 that the sample fiber presents weak birefringence in the visible light and near infrared region due to larger holes diameter and relative holes spacing. The calculated mode profiles of the other two groups are also indicated in Figs. 4(b) and (c), respectively, which show the same structure corresponding to Figs. 3(b) and (c). It should be pointed out that, the refractive index of either mode between the two modes in each group is equivalent. That is, the two modes in each group are degenerated. In each group, we observed that the two modes were orthogonally polarized and this is consistent with the experimental results.

In conclusion, we have successfully fabricated a mPOF with elliptical core by adopting in-situ chemical polymerization technology and the secondary sleeving draw-stretching technique. Microscope photography demonstrates the clear hole-structure retained in the fiber. Experiments of guided mode indicate that light can be strongly confined to the elliptical core region, and modal fields show distinct split as well as multi-mode characteristic. Adopting the measured parameters of real fiber, the cut-off wavelength was estimated and the guided mode fields were simulated by using FV-PWM, which were consistent with the experiment result. This fiber has strong multimode in the visible and near-infrared and it is possible to give weak birefringence due to twofold symmetry in structure. This kind of fiber is likely to be applied to achieve the fiber mode converters, mode

selective couplers and so on.

This work was supported by the National Natural Science Foundation of China under Grant No. 60437020. And the authors give many thanks to Australian Photonics Cooperative Research Centre, Optical Fiber Technology Centre, University of Sydney for helpful discussion. Y. Zhang's e-mail address is zhangyn@opt.ac.cn.

References

1. J. C. Knight, T. A. Birks, P. St. J. Russell, and D. M. Atkin, *Opt. Lett.* **21**, 1547 (1996).
2. T. A. Birks, J. C. Knight, and P. St. J. Russell, *Opt. Lett.* **22**, 961 (1997).
3. T. M. Monro, D. J. Richardson, N. G. R. Broderick, and P. J. Bennett, *J. Lightwave Technol.* **17**, 1093 (1999).
4. W. H. Reeves, J. C. Knight, and P. St. J. Russell, *Opt. Express* **10**, 609 (2002).
5. A. Ortigosa-Blanch, J. C. Knight, W. J. Wadsworth, J. Arriaga, B. J. Mangan, T. A. Birks, and P. St. J. Russell, *Opt. Lett.* **25**, 1325 (2000).
6. W. N. Macpherson, M. J. Gander, R. McBride, J. D. C. Jones, P. M. Blanchard, A. H. Burn Greenaway, B. Mangan, T. A. Birks, J. C. Knight, and P. St. J. Russell, *Opt. Commun.* **193**, 97 (2001).
7. W. E. P. Padden, M. A. van Eijkelenborg, A. Argyros, and N. A. Issa, *Appl. Phys. Lett.* **84**, 1689 (2004).
8. Y. Li, Q. Wang, and M. Hu, *Chin. Opt. Lett.* **1**, 570 (2003).
9. M. A. van Eijkelenborg, M. C. J. Large, A. Argyros, J. Zagari, S. Manos, N. A. Issa, I. Bassett, S. Fleming, R. C. McPhedran, C. M. de Sterke, and N. A. P. Nicorovici, *Opt. Express* **9**, 319 (2001).
10. A. Argyros, I. M. Bassett, M. A. van Eijkelenborg, M. C. J. Large, J. Zagari, N. A. P. Nicorovici, R. C. McPhedran, and C. Martijn de Sterke, *Opt. Express* **9**, 813 (2001).
11. G. Barton, M. A. van Eijkelenborg, G. Henry, M. C. J. Large, and J. Zagari, *Opt. Fiber Technol.* **10**, 325 (2004).
12. L. Wang, Y. Zhang, L. Ren, X. Wang, T. Li, B. Hu, Y. Li, W. Zhao, and X. Chen, *Chin. Opt. Lett.* **3**, S94 (2005).
13. Y. Zhang, K. Li, L. Wang, L. Ren, W. Zhao, R. Miao, M. C. J. Large, and M. A. van Eijkelenborg, *Opt. Express* **14**, 5541 (2006).
14. J. Zagari, A. Argyros, N. A. Issa, G. Barton, G. Henry, M. C. J. Large, L. Poladian, and M. A. van Eijkelenborg, *Opt. Lett.* **29**, 818 (2004).
15. T. M. Monro, D. J. Richardson, N. G. R. Broderick, and P. J. Bennett, *J. Lightwave Technol.* **18**, 50 (2000).
16. N. A. Mortensen, M. D. Nielsen, J. R. Folkenberg, A. Petersson, and H. R. Simonsen, *Opt. Lett.* **28**, 393 (2003).